

## Effects of Wheel Polygon on the Underground Train-Induced Vibration in a Building

Wang, Li; He, Chunyan; Zhu, Bin; Li, Zili

**DOI**

[10.1007/978-3-031-66971-2\\_119](https://doi.org/10.1007/978-3-031-66971-2_119)

**Publication date**

2024

**Document Version**

Final published version

**Published in**

Advances in Dynamics of Vehicles on Roads and Tracks III

**Citation (APA)**

Wang, L., He, C., Zhu, B., & Li, Z. (2024). Effects of Wheel Polygon on the Underground Train-Induced Vibration in a Building. In W. Huang, & M. Ahmadian (Eds.), *Advances in Dynamics of Vehicles on Roads and Tracks III: Proceedings of the 28th Symposium of the International Association of Vehicle System Dynamics, IAVSD 2023, Rail Vehicles* (pp. 1151-1160). (Lecture Notes in Mechanical Engineering). Springer. [https://doi.org/10.1007/978-3-031-66971-2\\_119](https://doi.org/10.1007/978-3-031-66971-2_119)

**Important note**

To cite this publication, please use the final published version (if applicable).  
Please check the document version above.

**Copyright**

Other than for strictly personal use, it is not permitted to download, forward or distribute the text or part of it, without the consent of the author(s) and/or copyright holder(s), unless the work is under an open content license such as Creative Commons.

**Takedown policy**

Please contact us and provide details if you believe this document breaches copyrights.  
We will remove access to the work immediately and investigate your claim.

***Green Open Access added to TU Delft Institutional Repository***

***'You share, we take care!' - Taverne project***

**<https://www.openaccess.nl/en/you-share-we-take-care>**

Otherwise as indicated in the copyright section: the publisher is the copyright holder of this work and the author uses the Dutch legislation to make this work public.



# Effects of Wheel Polygon on the Underground Train-Induced Vibration in a Building

Li Wang<sup>1</sup>  , Chunyan He<sup>1</sup>, Bin Zhu<sup>2</sup>, and Zili Li<sup>1</sup> 

<sup>1</sup> Section of Railway Engineering, Delft University of Technology, Delft 2628CN, The Netherlands

[l.wang-7@tudelft.nl](mailto:l.wang-7@tudelft.nl)

<sup>2</sup> China Academy of Railway Sciences Corporation Limited, Beijing 100081, China

**Abstract.** Excessive underground train-induced building vibration is an environmental concern resulting in human distress. Wheel polygon is probably one of the main vibration sources. In the present work, an explicit-integration time-domain, fully coupled 3D dynamic train-track-tunnel-soil-building FE model is developed and employed to investigate the effects of wheel polygon on the building vibration. Measured wheel polygon data is analyzed and input into the developed FE model. Based on the simulation results, it is found that the contribution of the wheel polygon to the building vibration is considerable in the frequency range from 30 to 180 Hz. Wheel polygon makes the building vibration more pronounced at the P2 resonance frequency and the passing frequencies ( $f = v/\lambda$ ) of wheel polygon. From the foundation to a high floor in the building, the effect of the P2 resonance-related wheel polygon attenuates the slowest while the effects of the other orders of wheel polygon attenuate fast.

**Keywords:** Wheel Polygon · Train-induced Building Vibration · Finite Element Modelling · Underground Train · Dynamic Interaction

## 1 Introduction

In recent years, excessive underground train-induced vibration in buildings becomes a major environmental problem [1]. Especially in mega cities with dense population, the residential buildings have to be very close to the metro lines in order to save land resource. The building vibration is perceived by humans in terms of the whole body vibration at low frequencies ranging from 1 Hz up to about 80 Hz and the structure-borne noise in the frequency range of about 16 Hz–250 Hz [2]. The allowable vibration levels in different city areas are specified in some standards [3, 4].

Wheel polygon is a common periodical non-uniform wear phenomenon occurring at wheel surface [5]. An extensive field test in Switzerland showed that wheel polygon is a key parameter influencing the ground vibration level [6]. Recent in-tunnel vibration monitoring tests in China showed that the vibration amplitude of the tunnel wall between 40 Hz and 160 Hz is directly affected by the severity of the wheel polygon, and the spectra peaks match well with the frequencies excited by the dominant wavelengths

of the wheel polygon [7]. The tunnel vibration propagates as waves travelling through the soil layers and being received by the building nearby. However, the relationship between the metro wheel polygon and the vibration in a building has scarcely been investigated. The present work explores numerically the contribution of wheel polygon to the underground train-induced vibration in a building.

To estimate and predict the underground train-induced vibration in buildings, and also to assess the effectiveness of a vibration mitigation measure, many models and methods have been developed [8], such as analytical methods [9, 10], 2.5D approaches [11, 12], and hybrid methods [13, 14]. To consider the complex geometries of the track structure and a typical multi-story building thus allowing the simulations more realistic and accurate, in the present work, an explicit-integration time-domain, fully coupled, 3D train-track-tunnel-soil layers-building finite element (FE) model is developed and validated with in situ tests data. Measured wheel polygon data is analyzed and input into the developed FE model. The effects of the wheel polygon on the underground train-induced vibration in a building are evaluated.

## 2 Methodology

### 2.1 Modelling and Validation of the 3D Train-Track-Tunnel-Soil Layers-Building FE Model

In the present model, as shown in Fig. 1, the two rails are modelled with beam elements and are extended at the two ends of the main part of the model in order to properly consider the approaching and leaving of a underground train which is about 120 m long. The underground train consists of 6 vehicles. The carbody, two bogies and the secondary suspensions of each vehicle are together lumped into 8 equal mass points. The 4 wheelsets of each vehicle are lumped into 8 mass points accordingly. The primary suspensions are modelled as springs and dampers connecting the 8 pairs of mass points. The track, tunnel, soil layers and the building are all modelled with 8-node solid finite elements. Their accurate geometries are considered where necessary.

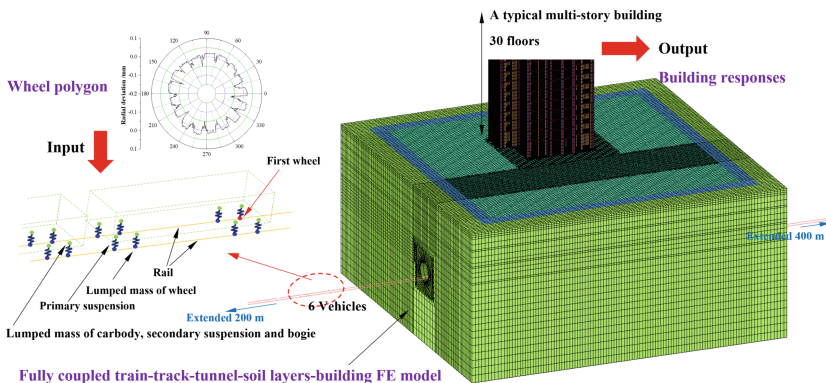


Fig. 1. Illustration of the methodology

The train and the track are fully coupled by properly considering the wheel-rail contact which is defined as the wheel mass points moving along the rails. The vertical contact force  $F$  is

$$F = K_H \cdot (Z_W - Z_R - \delta) \quad (1)$$

where  $K_H$  is the contact stiffness,  $Z_W$  is the displacement of wheel,  $Z_R$  is the displacement of rail, and  $\delta$  is the radial deviation of the input wheel polygon. A linear contact

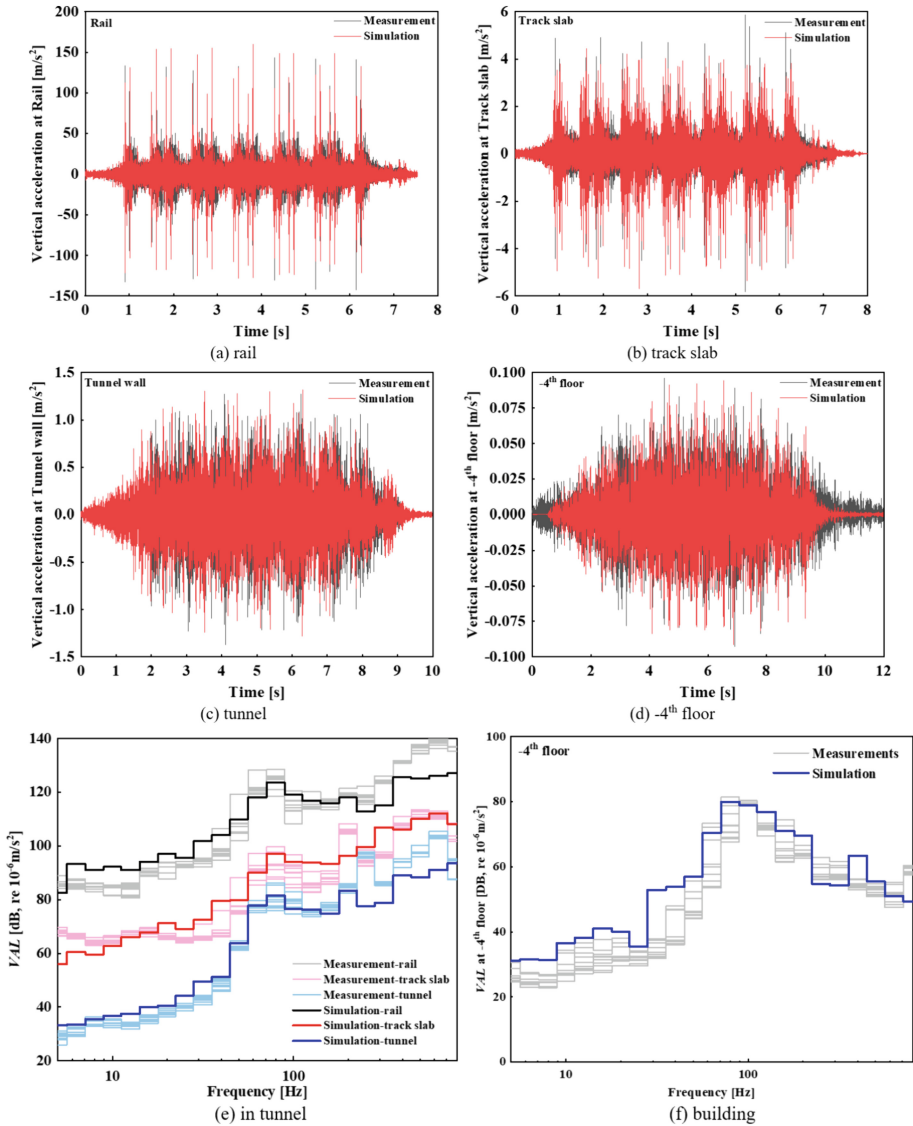


Fig. 2. Validation of the model by comparing measurements and simulations

stiffness of  $1.32\text{E}9$  N/m is assumed [15], while no tensile force is generated when the wheel loses contact with the rail.

The model is validated by comparing the simulated and the measured train-induced responses at the rail, track slab, tunnel wall and the building. As shown in Fig. 2.

In general, good agreements between the numerical and experimental results have been achieved both in time domain and frequency domain. Thus, the model is capable of simulating the vibration transfer from the underground train to a typical building nearby.

## 2.2 Wheel Polygon as Input

### 2.2.1 Measurement of Wheel Polygon

The roughness of all the 48 wheels of a typical Chinese underground train (Type B) is measured. The accumulated operation mileage is up to 238,000 km. Several wheels are found with polygonization.

Wheel polygon is characterized in different orders, i.e., the number of waves along the wheel circumference. Figure 3 shows the measured radial deviation of a typical wheel with wheel polygon. The 6<sup>th</sup> and 10<sup>th</sup> order wheel polygon are extracted from the complete measurement for comparison analysis.

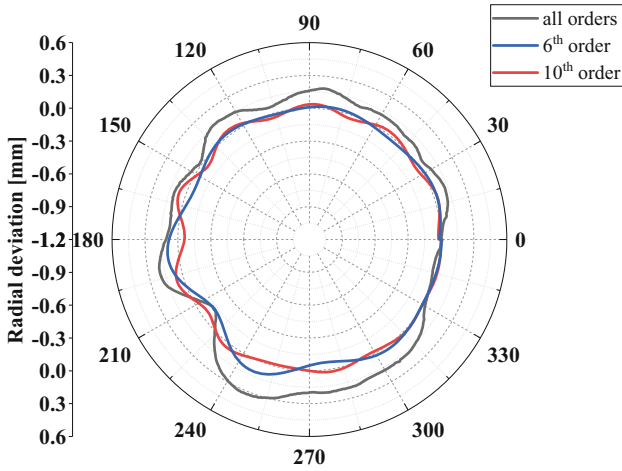
It can be seen in Fig. 3(a) that the maximum radial deviation of the wheel roughness is about 0.32 mm. The maximum radiation deviations of extracted wheel roughness with only the 6<sup>th</sup> and the 10<sup>th</sup> order wheel polygon are about 0.12 mm and 0.065 mm, respectively. The wavelength contents of the wheel roughness are shown in Fig. 3(b). The wheel diameter is 0.83 m, thus the wavelengths of the 6<sup>th</sup> and 10<sup>th</sup> order wheel polygon are 0.436 m and 0.261 m, respectively.

### 2.2.2 Considerations of Wheel Polygon in the Simulations

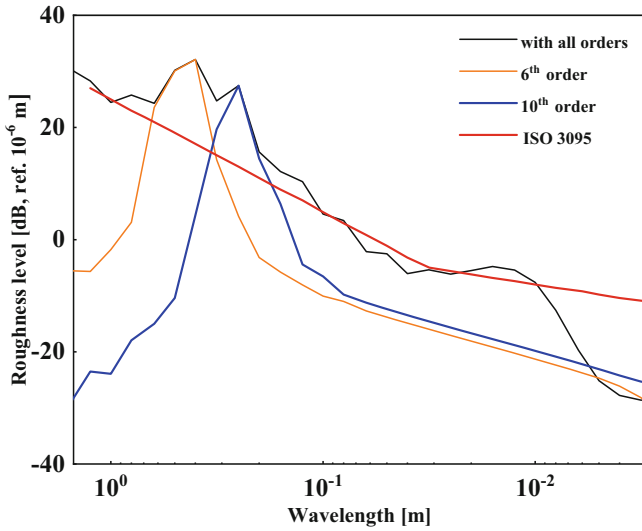
The wheel polygon is the input to the model in this study. Since the wheels are lumped into mass points, the wheel rotation cannot be considered. To consider the periodical effect, for each wheel, the measured wheel polygon along a complete circumference should be repeated along the train's moving direction.

To simplify the problem and also quantify the contribution of a single wheel with polygon to the whole building response, only one wheel is considered with wheel polygon in this study. The other wheels are all perfectly smooth. The rail surface is also perfectly smooth. The track irregularity is not considered. The following cases are considered, as listed in Table 1.

The train speed is 75 km/h in the simulations. The parameters of the vehicles, track, tunnel, soil layers and the building are listed in Tables 2 and 3.



(a) Radial deviation of the measured wheel polygon and its extractions



(b) Roughness level of the wheel polygon [16]

**Fig. 3.** Measured radial deviation of a typical wheel with wheel polygon

**Table 1.** Wheel polygon cases considered in the simulations

Case No	Considered wheels	Wheel polygon
1	No	No
2	Only 1 <sup>st</sup> wheel* of the 1 <sup>st</sup> vehicle	All orders

(continued)

**Table 1.** (continued)

Case No	Considered wheels	Wheel polygon
3	Only 1 <sup>st</sup> wheel of the 1 <sup>st</sup> vehicle	Order 6
4	Only 1 <sup>st</sup> wheel of the 1 <sup>st</sup> vehicle	Order 10

\* the 1<sup>st</sup> wheel refers to the left wheel of the front wheelset of the 1<sup>st</sup> vehicle, as shown in Fig. 1 (see the wheel colored in red). Left side of the track is the side closer to the building.

**Table 2.** Parameters of a vehicle

	Mass [kg]	Stiffness [N/m]	Damping [N.s/m]
Carbody	49700	/	/
Bogie	3740	/	/
Wheelset	1530	/	/
Primary suspension	/	1.3E6	1.3E4

**Table 3.** Parameters of the track, tunnel, soil layers and the building

		Elastic modulus [MPa]	Poisson's ratio	Density [kg/m <sup>3</sup> ]	Rayleigh damping	
					$\alpha$ [s <sup>-1</sup> ]	$\beta$ [s]
Rail		2.06E5	0.3	7800	/	/
Track slab		3.45E4	0.2	2350	0	0.0001
Adjusting layer		2.0E3	0.2	1900	0	0.0005
Base		3.0E4	0.2	2200	0	0.0002
Tunnel		3.4E4	0.2	2400	0	0.0001
Soil layers	1 <sup>st</sup> layer	422	0.47	1900	0.1	0.04
	2 <sup>nd</sup> layer	356	0.47	2100	0.1	0.04
	3 <sup>rd</sup> layer	577	0.47	2050	0.1	0.04
	4 <sup>th</sup> layer	994	0.47	2210	0.1	0.04
	5 <sup>th</sup> layer	1365	0.47	2300	0.1	0.06
Building	Floors	28000	0.2	2000	0	0.01
	Walls	30000	0.2	2100	0	0
	Foundation	32000	0.2	2400	0	0.01

### 3 Results and Discussions

#### 3.1 Effects of Wheel Polygon on the Vibration at the Building Foundation

The effects of the wheel polygon with various orders on the vibration at the building foundation are investigated, as shown in Fig. 4.

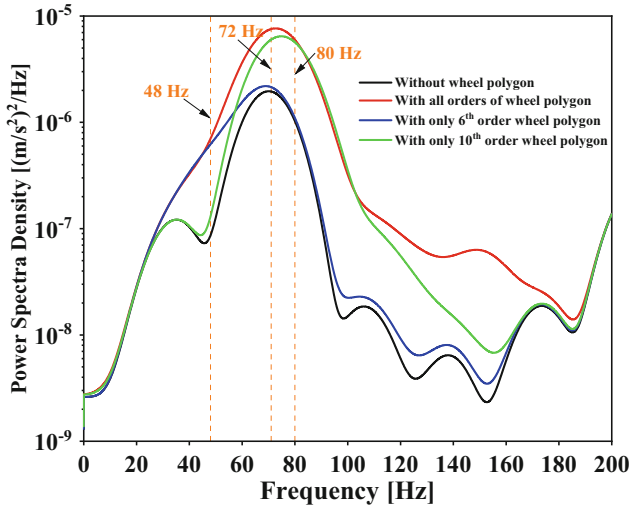


Fig. 4. Vibration at the building foundation

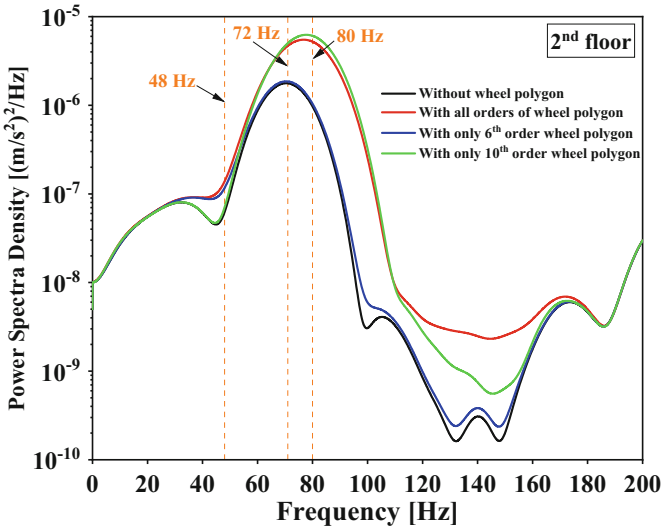
It can be seen in Fig. 4 that, without wheel roughness (the black solid line), the main spectral peak of the vibration is at about 72 Hz which is determined by the P2 resonance. When the measured wheel roughness with complete orders of wheel polygon is the input, the vibration at the building foundation is stronger in the frequency range from about 30 to 180 Hz, as shown with the red solid line in Fig. 4. The main spectral peak is still at about 72 Hz and dominant.

The extracted 6<sup>th</sup> and 10<sup>th</sup> order wheel polygons can also result in stronger vibration compared with the case without wheel roughness, as shown with the blue and green solid lines in Fig. 4, respectively. Both of them also present main spectral peaks at about 72 Hz. Moreover, the 6<sup>th</sup> order wheel polygon results in higher frequency content at about 48 Hz, which matches well with the value of the train speed divided by the wavelength of the 6<sup>th</sup> order wheel polygon. The same happens to the 10<sup>th</sup> order wheel polygon.

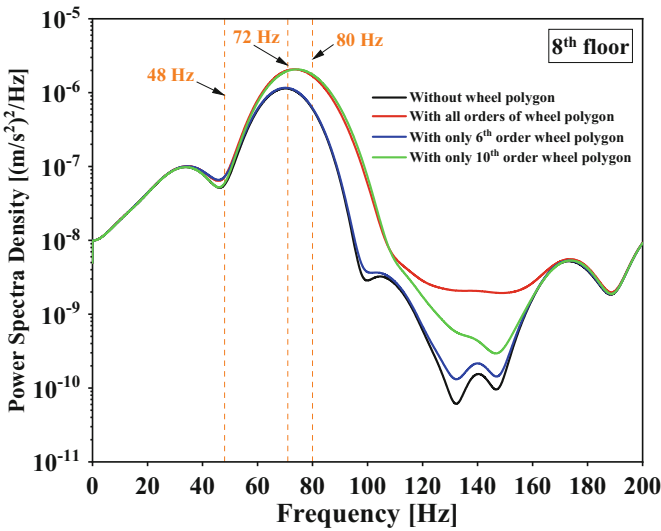
#### 3.2 Effects of Wheel Polygon on the Vibration at Building Floors

The effects of the wheel polygon on the vibration at the building floors are investigated. Take the 2<sup>nd</sup> and the 8<sup>th</sup> floor as examples, as shown in Fig. 5.

It can be seen in Fig. 5 that, compared with that at the building foundation, the vibrations at building floors show similar frequency contents within 200 Hz, and are



(a) Vibration at the 2<sup>nd</sup> floor



(b) Vibration at the 8<sup>th</sup> floor

**Fig. 5.** Wheel polygon-induced vibration at the building floors

getting lower in amplitudes due to the building structural damping. But the main spectral peaks remain at 72 Hz.

From Figs. 4 and 5, it can also be found that, from the foundation to the high floors, the red solid line becomes closer to the black solid line, which indicates that the contribution of the wheel polygon to the building vibration becomes smaller. Moreover, the blue line becomes closer to the black line while the green line becomes closer to the red line. It indicates that the contribution of the extracted 6<sup>th</sup> order wheel polygon attenuates much

faster than that of the 10<sup>th</sup> order wheel polygon. When it is at the 8<sup>th</sup> floor (see Fig. 5(b)), almost only the contribution of the 10<sup>th</sup> order wheel polygon remains. The 10<sup>th</sup> order wheel polygon provides an exciting frequency closer to the P2 resonance frequency, thus it is probably that the P2 resonance related wheel polygon contributes the most to the building vibration.

## 4 Conclusions and Future Works

In the present work, an explicit-integration time-domain, fully coupled 3D dynamic train-track-tunnel-soil-building FE model is developed and employed to investigate the effects of wheel polygon on the building vibration induced by underground trains.

It is found that the contribution of the wheel polygon to the building vibration is considerable in the frequency range from 30 to 180 Hz. Wheel polygon makes the building vibration more pronounced at the P2 resonance frequency and the passing frequencies ( $f = v/\lambda$ ) of wheel polygon. The effect of the P2 resonance-related wheel polygon attenuates the slowest when the vibration propagates from the foundation to a high floor in the building.

It is worthy to note that, the results are obtained considering only one wheel with polygon. In the future, the effects of the rail roughness and the track irregularities, especially combined with the wheel polygon should be investigated as well, so as to make the contributions of the wheel and rail or track to the building vibration more clear, thus a better maintenance strategy involves various vibration mitigation measures, such as wheel reprofiling and rail grinding, could be developed.

## References

1. Connolly, D.P., Marecki, G.P., Kouroussis, G., Thalassinakis, I., Woodward, P.K.: The growth of railway ground vibration problems - a review. *Sci. Total Environ.* **568**, 1276–1282 (2016)
2. Thompson, D.J., Kouroussis, G., Ntotsios, E.: Modelling, simulation and evaluation of ground vibration caused by rail vehicles. *Veh. Syst. Dyn.* **57**(7), 936–983 (2019)
3. DIN 4150 - 3 - 1999. Vibrations in buildings - Part 3: Effects on structures
4. GB 10070 - 88. Standard of environmental vibration in urban area. (In Chinese)
5. Tao, G.Q., Wen, Z.F., Jin, X.S., Yang, X.X.: Polygonisation of railway wheels: a critical review. *Railw. Eng. Sci.* **28**, 317–345 (2020)
6. Nielsen, J.C.O., et al.: Reducing train-induced ground-borne vibration by vehicle design and maintenance. *Int. J. Rail Transport.* **3**(1), 17–39 (2015)
7. Ma, M., Li, M.H., Qu, X.Y., Zhang, H.G.: Effect of passing metro trains on uncertainty of vibration source intensity: monitoring tests. *Measurement* **193**, 110992 (2022)
8. Sheng, X.Z.: A review on modelling ground vibrations generated by underground trains. *Int. J. Rail Transport.* **7**(4), 241–261 (2019)
9. Trochides, A.: Ground-borne vibrations in buildings near subways. *Appl. Acoust.* **32**(4), 289–296 (1991)
10. He, C., Zhou, S.H., Guo, P.J.: An efficient three-dimensional method for the prediction of building vibrations from underground railway networks. *Soil Dyn. Earthq. Eng.* **139**, 106269 (2020)
11. Yang, Y.B., Hung, H.H.: Soil vibrations caused by underground moving trains. *J. Geotech. Geoenvironmental Eng.* **134**(11), 1633–1644 (2008)

12. Qu, S., Yang, J.J., Zhu, S.Y., Zhai, W.M., Kouroussis, G.: A hybrid methodology for predicting train-induced vibration on sensitive equipment in far-field buildings. *Transport. Geotechnics* **31**, 100682 (2021)
13. Yang, J.J., et al.: Prediction and mitigation of train-induced vibrations of large-scale building constructed on subway tunnel. *Sci. Total Environ.* **668**, 485–499 (2019)
14. Colaço, A., Barbosa, D., Costa, P.A.: Hybrid soil-structure interaction approach for the assessment of vibrations in buildings due to railway traffic. *Transportation Geotechnics* **32**, 100691 (2022)
15. Wang, L., Wang, P., Wei, K., Dollevoet, R., Li, Z.: Ground vibration induced by high speed trains on an embankment with pile-board foundation: Modelling and validation with in situ tests. *Transportation Geotechnics* **34**, 100734 (2022)
16. ISO 3095 - 2013. International Standard: Acoustics - Railway applications - Measurement of noise emitted by railbound vehicles